Research Journal of Chemical Sciences ISSN 2231-606X
Vol. **9(3),** 24-39, July **(2019)** *Res. J. Chem. Sci.*

Octahedral platinum (IV) complexes of mixed piperaquine, sulfadoxine and pyrimethamine: synthesis, spectroscopy, antioxidant and antibacterial studies

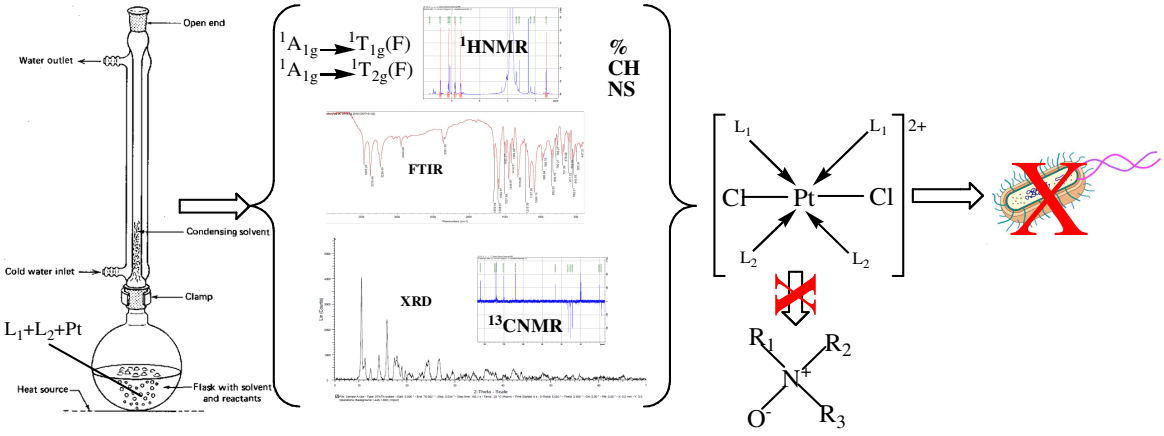
Ayipo Yusuf Oloruntoyin[1*], Osunniran Wahab Adesina[1], Obaleye Joshua Ayoola[2], Badeggi Umar Muhammad[3] and Ayinde Monsurat Olabisi[1]

[1]Department of Chemical, Geological and Physical Sciences, Kwara State University, Malete, Nigeria
[2]Department of Chemistry, University of Ilorin, Ilorin, Nigeria
[3]Department of Chemistry, Cape Pennisula University of Technology, Cape Town, South Africa
yusuf.ayipo@kwasu.edu.ng

Available online at: www.isca.in, www.isca.me
Received 28th February 2019, revised 12th May 2019, accepted 5th July 2019

Abstract

Synthesis of coordination compounds of Pt (IV) with mixed piperaquine-sulfadoxine and piperaquine-pyrimethamine has been carried out by 1:1:1 stochiometry ratio of ligands to metal ion. Characterization of the synthesized complexes was carried out using solubility evaluation, determination of melting point, elemental analysis, UV-visible spectrophotometry, FTIR, ^{1}H NMR, ^{13}C NMR, DEPT-135 and XRD spectroscopy. FTIR spectral data suggest that all the ligands behaved as bidendate ligands with pyrimethamine coordinates to the metal centre through (N-H) and (C-Cl); sulfadoxine through (N-H) and (S=O); piperaquine through (N-H) and (C-Cl). The electronic spectra also revealed that the metal center moiety is six-coordinate with octahedral geometry. The XRD data obtained established the crystal profile and novelty of the metal complexes synthesized. Antioxidant studies carried out using DPPH with ascorbic acid as standard shows metal complexes to be promising antioxidant agents with the IC_{50} values of 543, 1031. In vitro antibacterial screening of the ligands and synthesized metal complexes were evaluated against Escherichia coli, Staphylococcus aureus and Bacteria anthrancitis using agar diffusion technique. The results obtained reveal that synthesized metal complexes showed enhanced antibacterial activities when compared to the parent ligands and compete well with oxytetracyclin, a renowned antibiotic.



L_1 = Piperaquine; L_2 = Sulfadoxine/Pyrimethamine

Keywords: Piperaquine, platinum (IV) complex, spectroscopy, X-ray diffraction, antioxidant, antibacterial.

Introduction

Piperaquine is an antimalarial, belonging to the quinoline group (bisquinoline) which was used in china as prophylaxis and treatment of malaria. The IUPAC name is 4-4'-(1,3-propanediyldir-4,1-piperanzindyl) bis (7-chloroquinoline). Its mode of action similar to that of chloroquine, however, it becomes an object of renewed interest in combination therapy with artemisinin derivatives due to its longer half-life (which prevents malaria recurrence) in human system[1-3].

Sulfadoxine is a broad spectrum sulfanaliamide and a synthetic analog of para aminobenzene (PABA) with bacteriostatic and antimalarial properties. The IUPAC name is 4-amino-N-(5,6-dimethoxy pyrimidin-4-yl) benzene sulphonamide[3,4].

Pyrimethamine is synthetically derived from ethyl-pyrimidine with potential antimalarial activities. It is a good inhibitor of dehydrofolate reductase, having the IUPAC name as 5-(4-Chlorophenyl)-6-ethyl-2,4-pyrimidinediamine[3].

Research works have revealed development in the application of transition metals complexes as therapy against human diseases. Transition metals in different oxidation states interact with many negatively charged molecules[5]. This properties foster the development of metal based coordination compounds with enhanced pharmacological and therapeutic applications[6,7].

In bioinorganic chemistry field, the unique properties of transition metal ions have been exploited for designing new chemotherapeutic agents with higher cytotoxicity. This has contributed to the discovery of new drugs for cancer treatment such as cisplatin[8,9]. Coordination compounds of transition metals are very useful in catalysis, synthesis of biomaterials, photochemistry and in biological systems due to variations in their chemical, magnetic and optical properties[6,10,11].

In furtherance of our studies of chelation of transition metals with biologically important ligands, we give an account of the synthesis, characterization, antioxidant and antibacterial studies of Platinum (IV) complexes of mixed piperaquine, sulfadoxine and pyrimethamine as reported by literatures[2,4,9,12] with modifications.

Materials and methods

Materials: The materials are used as commercially obtained without further purification. They include Platinum (IV) chloride hexahydrate, Ethanol, Acetone, DMSO, Lactic acid, Acetic anhydride from Sigma Aldrich. The ligands (piperaquine and sulfadoxine/pyrimethamine) are obtained from Zuhai Rundu Pharmaceuticals, China and Sam Pharmaceuticals, Nigeria respectively.

Ligands

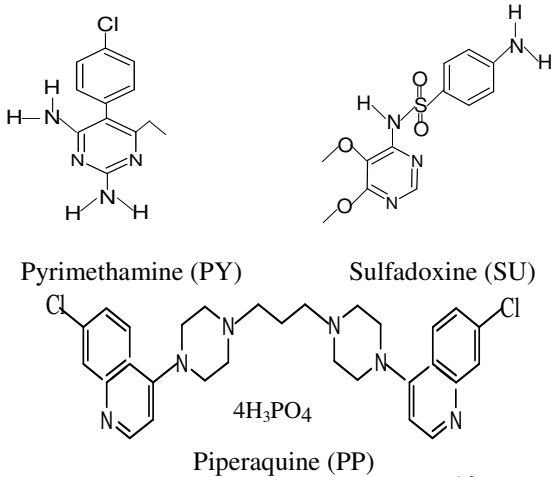


Figure-1: Molecular structures of ligands[1,3].

Preparation of the complexes: Synthesis of $[Pt(PP)(PY)Cl_2]Cl_2.4H_3PO_4.6H_2O$: 0.49g (0.002mol) of pyrimethamine and 1.07g (0.002mol) of piperaquine was each dissolved in 20mL of 5% w/v Lactic acid. The solutions were added and refluxed in a water bath (at 70°C) for 10 minutes for a complete dissolution of piperaquine. 20mL of 0.0193 $moldm^{-3}$ of $H_2PtCl_6.6H_2O$ was then added to the mixture, while the refluxing process continued for another 2 hours when a stable yellow precipitate was formed. The crystals were filtered, washed using 5% w/v Lactic acid then distilled water.

Mol. Wt 1652.26g/mol, Yield 1.92g(58%), Anal. Calcd. (Found)% ($C_{43}H_{76}Cl_7N_{10}O_{22}P_4Pt$) C 31.26(30.36), H 4.64(4.35), N 8.76(9.30), Pt 11.81. ^{1}H NMR (d_6-DMSO, 400 MHz) 8.82 (d, J=7.2Hz), 8.45(s), 8.24(d, J=12.4 Hz), 8.11(d, J =8.7Hz), 7.75 (d, J=9.2Hz), 7.62 (d, J=10Hz), 7.35 (d, J = 7.2Hz), 6.58 (d, J = 8.4Hz), 3.90 (s), 3.71(br,s), 1.22(t)ppm. ^{13}C NMR (d_6-DMSO, 400 MHz) δ: 18.61, 20.86, 31.13, 48.59, 49.06, 50.85, 53.19, 54.45, 60.65, 107.76, 112.92, 115.90, 118.55, 120.23, 125.87, 127.17, 127.77, 128.20, 128.87, 130.23, 138.62, 140.55, 144.02, 150.99, 151.15, 153.12, 160.79, 161.84, 163.58ppm.

Synthesis of $[Pt(PP)(SU)Cl_2]Cl_2.4H_3PO_4.6H_2O$:0.62g (0.002 mol) of sulfadoxine and 1.07g (0.002 mol) of piperaquine was dissolved in 20mL of acetone and 20mL of hot distilled water respectively. The solutions were mixed by swirling in water bath for 5minutes while 20mL of 0.0193$moldm^{-3}$ of $H_2PtCl_6.6H_2O$ was gently added and the mixture was refluxed for 3 hours until a stable yellow precipitate was obtained. The precipitate was filtered, washed using acetone, then distilled water and gently dried.

Mol. Wt 1387.51g/mol, Yield 1.25g(45%), Anal. Calcd. (Found)% ($C_{35}H_{59}Cl_6N_6O_{22}P_4PtS$) C 29.76(30.54), H 4.16 (4.35), N 8.26(8.69), Pt 11.51, S 1.89(1.99). ^{1}HNMR (d_6-DMSO, 400 MHz) δ: 9.58 (b, s), 8.82 (d, J = 7.2Hz), 8.24 (d, J = 12.4Hz), 8.13(s), 7.76 (d, J=8.8 Hz), 7.36 (d, J = 8.4Hz), 1.23 (d, J=6.8Hz), 3.74 (s, OCH_3), ^{13}CNMR (d_6-DMSO, 400 MHz) δ: 18.6, 20.9, 48.6, 50.8, 53.2, 66.2, 107.8, 118.6, 120.3, 127.8, 128.9, 138.6, 140.6, 144.1, 160.8, 176.8ppm.

Physical Measurements: The decomposition temperature and melting point of the metal-ligand chelates were determined using Gallenkamp melting point apparatus. Solubility of the ligands and metal complexes wer tested in Acetone, Lactic acid, distilled water, dimethylsulfoxide, acetic anhydride and aqua ethanolic solution while the ionic properties of the complexes were determined using Conductivity meter CDM 210, MeterLab.

Elemental analysis: Percentage by mass of CHNS elemental as well as Pt in the metal complexes was determined using the Vario El Cube Elemental Analyzer at the University of Western Cape, South Africa.

Spectroscopy: Fourier transform infrared spectroscopy: Powdered ligands and the metal complexes was loaded on Thermos Scientific Nicolet i5 Spectrophotometer FTIR

(Schimadzu, Japan), with a scan from 400-4000cm^{-1} with a Resolution of 4cm^{-1} equipped with KBr pellets carried out at the Kwara State University, Nigeria.

UV-visible spectroscopy: The electronic spectroscopy of the metal complexes in DMSO was carried out in the range 190-900 nm on Perkin Elmer ♪20 spectrophotometer. Quartz cuvettes of 1 cm path length was used as a holder and the analysis was obtained at the University of Lagos, Nigeria.

Xray diffraction spectroscopy: It was conducted at Department of Nuclear Physics, iThemba LABS , South Africa using D8 Advanced diffractometer, with the measurement of continuous ϑ-ϑ scan in locked coupled mode having a tube of Cu-Kα radiation ($\lambda K\alpha_1$=1.5406Å) and detector of LynxEye (Position sensitive detector).

^{1}HNMR, ^{13}CNMR and DEPT-135 NMR Spectroscopy: Nuclear magnetic resonance (NMR) spectroscopy NMR spectra were recorded at 25˚C, using deuterated Dimethyl sulfoxide (d_6-DMSO) as solvent, on a Bruker Avance 400MHz NMR spectrometer (Germany) at The University of the Western Cape, South Africa. The chemical shifts of ^{1}H (δH) and ^{13}C (δC) and DEPT-135 (δC)ppm were determined relative to tetramethylsilane as internal reference.

Determination of water of crystallization: Water of crystallization in the complexes is estimated by heating the sample to a constant weight, testing the gas evolved with cobalt (II) chloride paper.

Test for Cl^- and PO_4^{3-} in the complexes: To the solutions of the each metal complex sample, aqueous silver nitrate was added in drops, then in excess. The amount of AgCl precipitated was measured. The resulting precipitate was then tested against ammonium hydroxide solution which confirms Cl^- [13]. To confirm PO_4^{3-}, to solution of each complex sample, few drops of magnesia (mixture of $MgCl_2$ and NH_4OH) solution were added in drops, then in excess[13].

Anti-oxidant screening: Evaluation of antioxidant activities of the Complexes was carried out with DPPH Antioxidant Assay. Determination of the free radical scavenging potential of the complexes was achieved by using DPPH (1,1-diphenyl-2-picrylhydrazyl) assay as reportedly modified[12]. Slight dilute solution of the complexes (1ml) was mixed with 3.0mL of 60µM DMSO and solution of DPPH; the mixture was kept in the dark cupboard for 30min, then the absorbance measurement at 517nm was carried out. The gradual reduction in the absorbance of $DPPH^-$ while adding test samples compared to the control (ascorbic acid) was applied to evaluate the percentage inhibition (% Inhibition) according to the following the equation:

$$\% \text{ Inhibition} = \frac{\text{Abs}_{\text{control}} - \text{Abs}_{\text{sample}}}{\text{Abs}_{\text{control}}} \times 100.$$

The concentration of fraction required for 50% scavenging activity, IC_{50}, was then deduced from the dose-inhibition linear regression equation of the complexes. The antioxidant property of metal complexes was determined by comparing their IC_{50} with that of ascorbic acid. The lower the IC_{50} of any compound to IC_{50} of ascorbic acid the higher the antioxidant activities of that compound and the higher the IC_{50} of a compound to IC_{50} of ascorbic acid the lower the antioxidant activities[14].

Antibacterial screening: Antibacterial potentials of the ligands and each synthesized complex were evaluated for their inhibitory potential using agar diffusion[11] against *Escherichia coli*, *staphylococcus aureus* and *Bacillus anthracitis* obtained from department of microbiology, Kwara State University, Nigeria. A 3.26g of Nutrient broth was poured into 250mL of water in standard flask, 9mL of the nutrient broth was measured in a test-tube. A sterile innoculating loop was used to pick the organism and introduced to the broth, incubated for 18hrs at 37°C. The Muller hilton agar was autoclaved for 1hr at 121°C. It was allowed to cool. It was poured into labelled plates in a safety chamber. Spirit lamp was lit into the safety chamber in other to purify it. Holes/wells were bored into the plates containing the agar on which the bacteria culture has been evenly spread for a fair growth. Five different concentrations of ligands and metal complexes prepared using DMSO were then introduced into the well. The diameter of inhibition zone was determined in mm after 24 hours of 37°C incubation.

Results and discussion

The molecular composition of the metal complexes was formulated on the basis of elemental analysis results which were found to be in close agreement with the calculated values. The metal complexes were formed by 1:1:1 molar ratio of ligands and platinum ion. The Presence of uncoordinated water molecules was verified by the use of cobalt (II) chloride paper and the amount of water of crystallisation present determined from the formula below after heating the samples to a constant weight in an oven.

$$\frac{\text{mass of anhydrous complex}}{\text{molecular mass of anhydrous complex}} = \frac{\text{mass of hydrated complex}}{\text{molecular mass of hydrated complex}}$$

The elemental analysis results showed that four chloride ions were present in each of molecular formulation of complexes. However, the qualitative chloride test carried out indicated that two chloride ions are outside the coordination sphere as two moles of AgCl were precipitated when $AgNO_3$ solution was added to each complexes. This showed that the remaining two chloride ions have coordinated to metal ion and hence not available for reaction with $AgNO_3$ solution. In same vein, a white precipitate of magnesium ammonium phosphate formed when magnesia (mixture of $MgCl_2$ and NH_4OH) solution was added to the metal complexes indicating the presence of phosphate ion in form of phosphoric acid outside the coordination sphere[15].

The solubility data, melting point, conductivity and colour of the metal complexes and the ligands are shown in Table-1. The metal complexes and the ligands were all soluble in DMSO because it is a polar aprotic solvent. The electronegative end of DMSO is able to interact with the cationic end of the complexes while the electropositive end interacts well with the anionic end of the complexes. The ionic properties of the complexes are confirmed by their conductivity results. The melting points and the colours of the metal complexes differed from those of the ligands, an insight into the formation of coordination compounds. The change in the solubility and melting point has contributed to the indication that a chemical reaction has occurred[2,8].

The characteristics FTIR bands of the ligands and metal complexes are presented in Table-2. The characteristics FTIR bands of the metal chelates differed from that of the free ligands either by a shift or disappearance of some characteristics frequency bands as a proof of coordination. The IR spectra of the ligands showed a medium intensity bands at 3465cm^{-1} and 3378cm^{-1} (sulfadoxine), 3433cm^{-1} and 3286cm^{-1} (piperaquine) and 3467cm^{-1} and 3310cm^{-1} (pyrimethamine) which could be assigned to N-H stretching frequency. These symmetric and asymmetric N-H stretching frequencies of the ligands shifted hypsochromically in the spectra bands of the metal complexes, thereby indicating the involvement of NH_2 in chelation[10,13] The disappearance of one the bands in the piperaquine-pyrimethamine metal complex is also a proof of coordination. The asymmetric and symmetric (S=O) band of sulfadoxine which was observed at 1384cm^{-1} and 1160cm^{-1} respectively shifted to higher frequency in the spectrum of metal complex suggesting its participation in coordination[2,7,8,15]. The FTIR data showed that each of the ligand acted bidentately coordinated to the metal ion through NH and C-Cl (pyrimethamine), NH and S=O(sulfadoxine), NH and C-Cl (piperaquine)[16]. The possibility of piperaquine acting as a bidentate ligand is confirmed by the separation, $\Delta\nu$ of the $\Delta\nu_{asy}$(N-H)–$\Delta\nu_{sym}$(N-H) of the ligand and those of the complexes (i.e. $\Delta\nu_L > \Delta\nu_C$), that of sulfadoxine through $\Delta\nu_{asy}$(S=O)–$\Delta\nu_{sym}$(S=O) of the ligand and its complex (i.e. $\Delta\nu_L > \Delta\nu_C$) and that of pyrimethamine through $\Delta\nu_{asy}$(N-H) – $\Delta\nu_{sym}$(N-H) of the ligand and its complex (i.e. $\Delta\nu_L > \Delta\nu_C$)[10,14].

Table-1: Some major physical characteristics of the ligands and metal complexes.

Ligands/ Complexes	Solubility						M.P./ D.T., °C	Cond. 10^{-4} Ω^{-1}cm^{-1}	Colour
	D. H_20	LA	AES	DMSO	Acetone	Acetic anhydride			
SU	PS	PS	PS	S	S	PS	190-193	-	White
PY	NS	S	PS	S	PS	S	231-234	-	White
PP	S+Δ	S+Δ	PS	S	PS	NS	249-252	-	Yellow
$[Pt(PP)(PY)Cl_2]Cl_2.4H_3PO_4.6H_2O$	NS	NS	NS	S	NS	NS	209-216	4.29	Yellow
$[Pt(PP)(PY)Cl_2]Cl_2.4H_3PO_4.6H_2O$	NS	NS	NS	S	NS	NS	250°C	3.86	Yellow

S = soluble, NS = not soluble, PS = partially soluble, Δ =heat, AES= aqua ethanolic solution, LA= lactic acid, D.H_2O =distilled water, DMSO= dimethyl sulfoxide.

Table-2: FTIR bands of the ligands and their complexes.

Ligands/Complexes	ν(N-H)asy (N-H)sym cm^{-1}	ν(O=S=O)asy (O=S=O)sym cm^{-1}	ν(C-N) cm^{-1}	ν(C-Cl) cm^{-1}	ν(M-N)/(M-O)/ (M-Cl) cm^{-1}
SU	3465 s 3378 s	1384 m 1160 m	1160 m 1214 m	-	-
PP	3433 s 3286 w	-	1167 m 1240 m	875 S,s 837 s	-
PY	3467 s 3310 s	-	1138 w 1233 w	747 m 723 w	-
$[Pt(PP)(PY)Cl_2]Cl_2.4H_3PO_4.6H_2O$	3251 m	-	1129 w 1214 w	820 s 767 s	530 w 435 w
$[Pt(PP)(SU)Cl_2]Cl_2.4H_3PO_4.6H_2O$	3377 s 3239 S,s	1319 s 1191 s	1158 S,s	853 s 831 s	544 w 508 w

S: strong; m: medium; b: broad, w: weak; s: sharp.

New bands of weak to medium intensity in the region 400-500 cm^{-1} in the spectra of complexes which provide direct evidence for complexation (metal – ligand bond) are assigned to coupled vibrations: ν(M-Cl/M-N/M-O)[10,17-19]. Considering the

participation of the ligands in the coordination as confirmed above, proposed structures of the complexes are shown as Figure-3 and 4.

The electronic spectra, magnetism, coordination geometry and hybridization of the complexes are contained in Table-3. The platinum (IV) complexes have a low–spin d^6 configuration and the highest filled level is $^2t_{2g}$ (xy, xz, yz). Thus, the ground state is diamagnetic and labelled $^1A_{1g}$ [20,21].

The electronic spectra of the ligands in DMSO exhibited transition at 202nm–286nm which were assigned to intra-ligand transitions ($n \rightarrow \sigma^*$ and $n \rightarrow \pi^*$) [15]. The electronic spectra of Platinum (IV) complexes shows two absorption bands each of which were assignable to $^1A_{1g} \rightarrow {}^1T_{1g}(F)$, $^1A_{1g} \rightarrow {}^1T_{2g}(F)$ transitions as shown in Table-3. Thus, suggesting an octahedral geometry around the Pt (IV) ions [19,21-24].

^{1}H, ^{13}C and DEPT-135 NMR Spectroscopy: Both the proton, Carbon 13 and DEPT 135 were carried out in deuterated DMSO at 400MHz. The H NMR spectrum shows that the signals are similar to those of the starting ligands due to chemical equivalence. However, slight differences of chemical shifts were observed downfield which may be due to coordination to the metal atom.

DEPT revealed the presence of methylene and methyl groups from both ligands in the aliphatic region of the spectrum. Another evidence of the involvement of the two ligands as well as possible complex formation was the presence of 10 quaternary carbon atoms which is obviously contributed by the piperaquine and pyrimethamine moieties (Figure-1). Consequently, signals at δ 118.6, 125.9, 127.2, 138.6, 140.6, 151.2, 153.1, 160.8, 161.8 and 163.6 ppm were unambiguously assigned to aromatic quaternary carbon atoms from both ligands.

The ^{1}H NMR spectrum of the complex of piperaquine and sulfadoxine, measured in dimethylsulphoxide (DMSO) shows sharp and well resolved signals at the aliphatic region. Among others, the signal at δ 3.74ppm indicates a proton from methoxy ($-OCH_3$) group and is assigned to the methoxy on the sulphadoxine moiety (Figure-2). This is corroborated by the signal at δ 66.29ppm on the C 13 NMR spectrum. There is no broad singlet peak from the spectrum meaning that the primary amino group might have participated in the coordination to the metal ion. However, the proton at position 2, in-between the two nitrogen on the ring gave a singlet at δ 9.58ppm. This value is close to that of a δ-position of pyridine which is about 8.5ppm but even more deshielded because it is sandwiched between two nitrogen in a conjugated system. Another singlet of chemical shift δ 8.13ppm can be assigned to the proton of the secondary amine in the sulphadoxine moiety. Other signals in the ranges of δ 7.36–7.76ppm and δ 8.24-8.82ppm were unambiguously assigned to the aromatic ring doublets arising from piperaquine (Figure-1) and sulphadoxine (Figure-1) moieties respectively.

From the DEPT 135 spectrum, signals at δ 18.6, 48.8, 50.8 and 54.4ppm were assigned to methylene protons in the aliphatic region. Interestingly, they are only found in the piperaquine (Figure-1) moiety. In the aromatic region, δ 118.6-176.8ppm were assigned for the two ligands[16,19,21,24].

Table-3: Electronic spectra, magnetic properties, geometry and hybridization of the complexes.

Compounds	λ_{max} (nm)	$\bar{\upsilon}$ (cm^{-1})	Transitions	$\mu_{eff\ (B.M)}$	Geometry	Hybridization
SU	202 271	49505 36900	$n \rightarrow \sigma^*$ $n \rightarrow \pi^*$	--------	-------	---------
PY	202 286	49505 34965	$n \rightarrow \sigma^*$ $n \rightarrow \pi^*$	--------	--------	-------
PP	202	49505	$n \rightarrow \sigma^*$	--------	--------	--------
$[Pt(PP)(PY)Cl_2]Cl_2.4H_3PO_4.6H_2O$	784 462 318	12755 21645 31447	$^1A_{1g} \rightarrow {}^1T_{1g}(F)$ $^{1A1}_{g} \rightarrow {}^1T_{2g}(F)$ Charge Transfer	Diamagnetic	Octahedral	d^2sp^3 (Low spin)
$[Pt(PP)(SU)Cl_2]Cl_2.4H_3PO_4.6H_2O$	648 472	15432 21186	$^1A_{1g} \rightarrow {}^1T_{1g}(F)$ $^1A_{1g} \rightarrow {}^1T_{2g}(F)$	Diamagnetic	Octahedral	d^2sp^3 (Low spin)

X-Ray Diffraction Spectroscopy

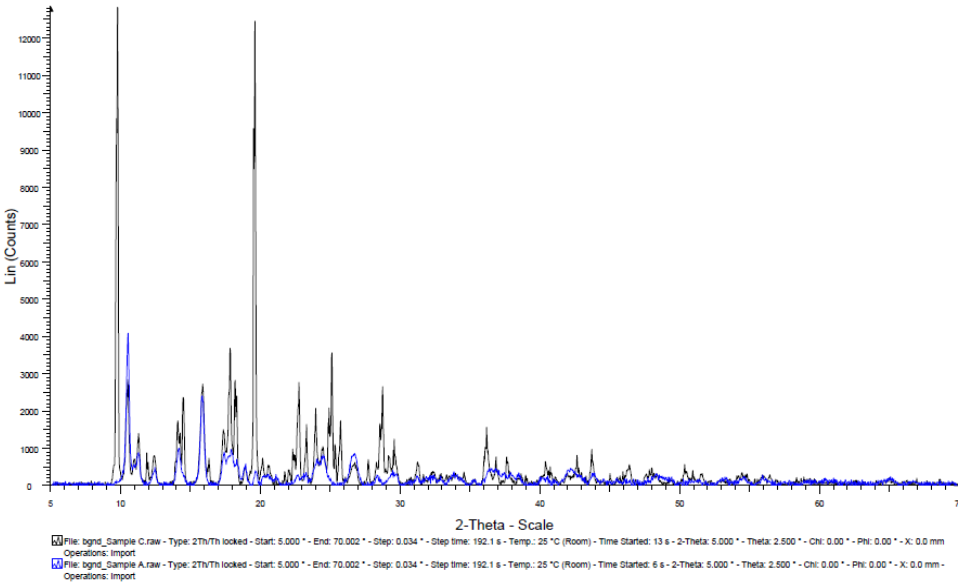


Figure-2: X-ray Diffractogram of $[Pt(PP)(PY)Cl_2]$ (sample A) and $[Pt(PP)(SU)Cl_2]$ (sample C).

Table-4: Phase Analysis: Miller Indexing, Interplanar Distances and Cubic Structures of $[Pt(PP)(PY)Cl_2]$.

2θ (obs.) (˚)	2θ(cal.) (˚)	d (obs.)	d (calc.)	I/I_0 (%)	$h^2 + k^2 + l^2$	hkl	Cubic System		
							SC	BCC	FCC
10.49	10.49	8.4264	8.4264	100	3	111	√	×	√
14.16	14.16	6.2496	6.2496	39	5	210	√	√	×
15.80	15.78	5.6112	5.6044	69	6	211	√	×	×
17.69	17.87	4.9585	5.0097	43	8	220	√	√	√
26.80	26.76	3.3289	3.3239	46	18	411, 330	√	√	×

Lattice Parameters: a = 25.28Å, b = 31.25Å, c = 33.61Å, Volume of Unit Cell = 26551.9(Å)^3 ; Type of Crystal System = Orthorhombic.

Table-5: Phase Analysis: Miller Indexing, Interplanar Distances and Cubic Sructures of $[Pt(PP)(SU)Cl_2]$.

2θ (obs.)	2θ(cal.)	d (cal.) (Å)	d (obs.) (Å)	I/I_0 (%)	$h^2 + k^2 + l^2$		Cubic System		
						hkl	SC	BCC	FCC
9.73	9.73	9.0828	9.0828	99.6	1	100	√	×	×
15.84	15.84	5.5904	5.5890	27.2	4	200	√	√	√
18.21	18.17	4.8784	4.8772	29.3	5	210	√	×	×
19.55	19.54	4.5371	4.5390	100.0	6	211	√	√	×
22.69	22.66	3.9158	3.9203	30.3	8	220	√	√	√
25.00	25.02	3.5590	3.5567	36.9	9	300, 221	√	×	×
28.64	28.65	3.1144	3.1134	30.7	12	222	√	√	√

Lattice Parameters: a=9.08Å, b=22.36Å, c=24.40Å, Volume of Unit Cell=4953.90(Å)^3; Type of Crystal System=Orthorhombic.

The XRD data presented in Tables-4,5 and Figure-2 revealed the diffraction pattern the complexes, the estimated Miller (hkl) indexing and the crystal structuresas reported by literatures[25,26]. The interplanar distances, "d" was estimated using Bragg's equation ($n\lambda = 2d \sin\theta$)[27]. The diffractograms indicate that the two complexes are polycrystallites in structure due to their peak

profiles[28]. The results in Table-5 confirm some of the crystals as simple, body-centred, face-centred cubic and overall orthorhombic[28-34]. The data also confirmed novelty of the complexes, i.e. different from those of the existing organic and inorganic compounds on the JCPDS files, as a supporting evidence of coordination[35,36].

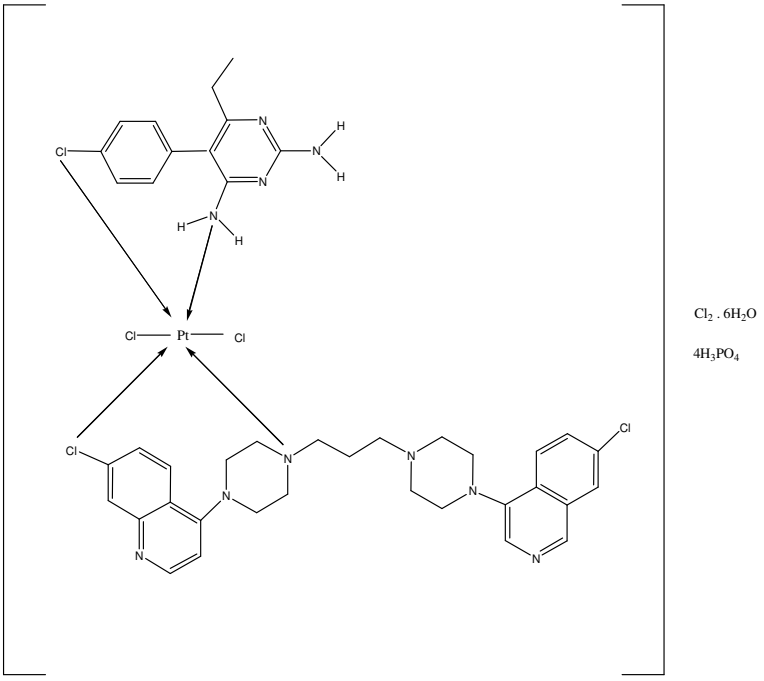


Figure-3: Proposed structure of $[Pt(PP)(PY)Cl_2]Cl_2.4H_3PO_4.6H_2O$.

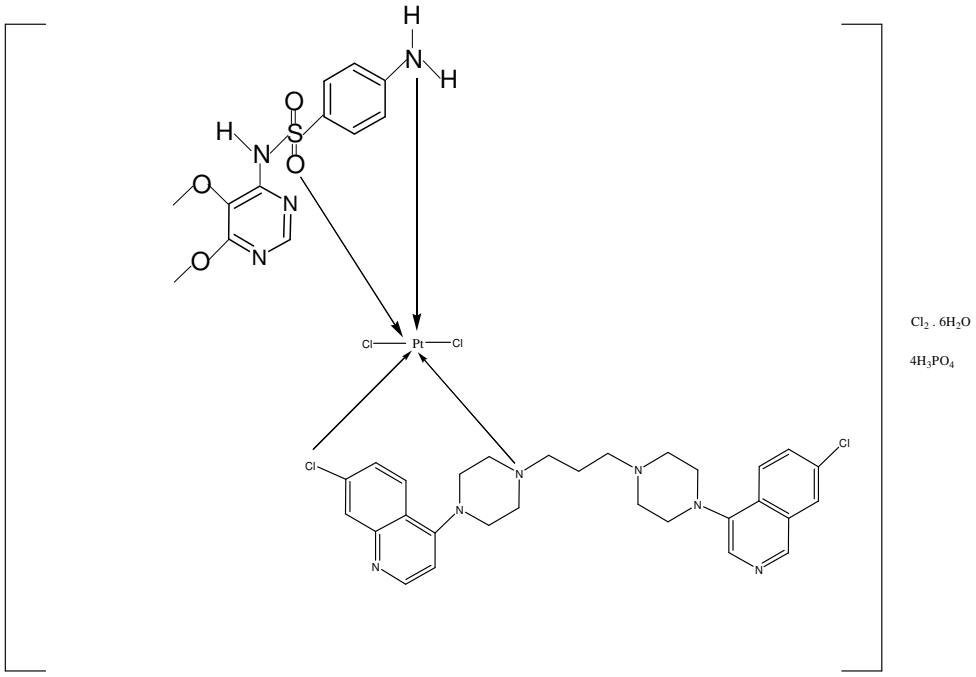


Figure-4: Proposed structure of $[Pt(PP)(SU)Cl_2]Cl_2.6H_2O.4H_3PO_4$.

The result of antioxidant evaluation of the synthesized metal complexes and the Ascorbic acid as a standard are contained in Table-6. The results reveal that the IC_{50} of synthesized metal complexes (543, 1031) are lower than that of ascorbic acid

(7526), hence have a very good antioxidant property[37,38]. The graphs of the antioxidant screening for the metal complexes and standard are shown in Figure-5 and 6.

Table-6: The result of antioxidant screening of the metal complexes and the standard (Ascorbic acid).

Conc. (ug/mL)	$[Pt(PP)(PY)Cl_2]Cl_2.4H_3PO_4.6H_2O$		$[Pt(PP)(SU)Cl_2]Cl_2.4H_3PO_4.6H_2O$		Ascorbic acid	
	A	% I	A	% I	A	%I
100	0.453 ± 0.003	514	0.574 ± 0.012	552	0.074 ± 0.003	87.18
200	0.525 ± 0.003	497	0.527 ± 0.003	499	0.079 ± 0.001	86.31
300	0.272 ± 0.000	209	0.486 ± 0.01	551	0.081 ± 0.003	85.96
400	0.205 ± 0.001	133	0.452 ± 0.015	414	0.084 ± 0.005	85.44
500	0.239 ± 0.004	172	0.361 ± 0.01	310	0.088 ± 0.005	84.75
IC_{50}	543		1031		7526	

A = Activity; %I = Percentage inhibition.

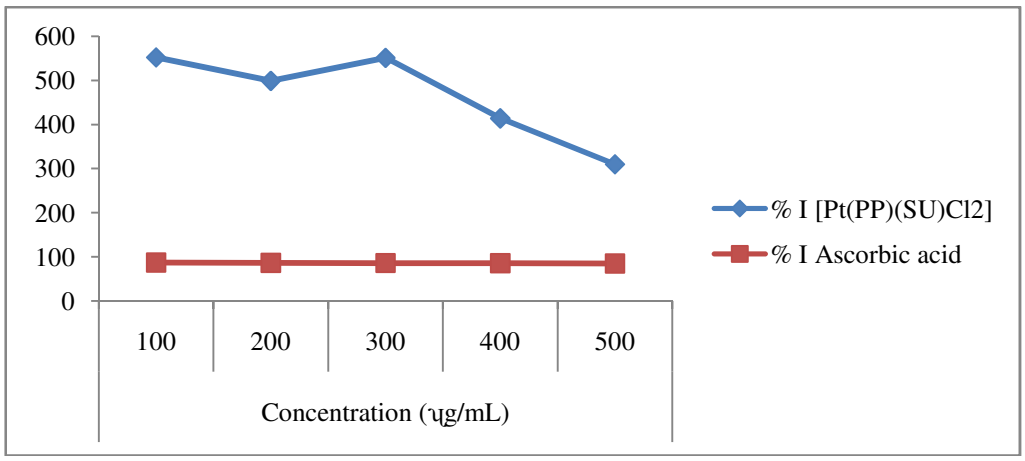


Figure-5: Graph of % inhibition against Concentration of $[Pt(PP)(PY)Cl_2]Cl_2.4H_3PO_4.6H_2O$.

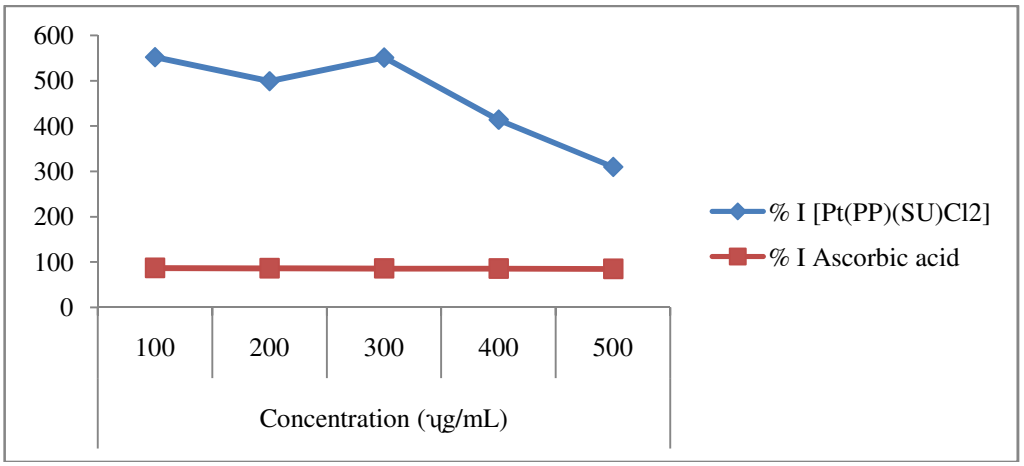


Figure-6: Graph of % inhibition against Concentration of $[Pt(PP)(SU)Cl_2]Cl_2.4H_3PO_4.6H_2O$.

Antibacterial screening result: The *in vitro* antibacterial screening results of the ligands and the synthesized complexes against *Escherichia coli*, *Bacillus anthracitis* and S*taphylococcus aureus* are reported in Table-7.

Table-7: Antibacterial potentials of the ligands and complexes

Sample	Conc. (%)	Inhibition Zone in *S. aueus* (mm)	Inhibition Zone in *E. coli* (mm)	Inhibition Zone in *B. Anthracis* (mm)
DMSO	-	00	00	00
PP	1	3.50	4.00	7.38
	2	3.82	4.00	8.10
	3	4.20	4.51	10.21
	4	4.73	4.95	10.64
	5	5.13	5.20	16.75
SU	1	5.20	5.25	5.32
	2	5.40	5.40	6.04
	3	6.25	6.26	6.20
	4	6.25	6.27	8.60
	5	6.30	6.35	12.88
$[Pt(PP)(PY)Cl_2]$	1	17.0	17.22	10.16
	2	18.0	18.21	12.11
	3	20.0	20.00	15.65
	4	23.0	23.54	17.33
	5	27.0	27.15	24.01
$[Pt(PP)(SU)Cl_2]$	1	14.0	16.11	18.30
	2	17.1	17.1	20.45
	3	18.6	18.6	26.79
	4	18.9	20.2	32.08
	5	19.20	21.0	34.83
Oxytetracyclin	1	15.39	25.00	14.90
	2	15.18	28.23	20.74
	3	16.94	32.36	24.55
	4	15.88	38.00	35.62
	5	20.56	38.10	35.81

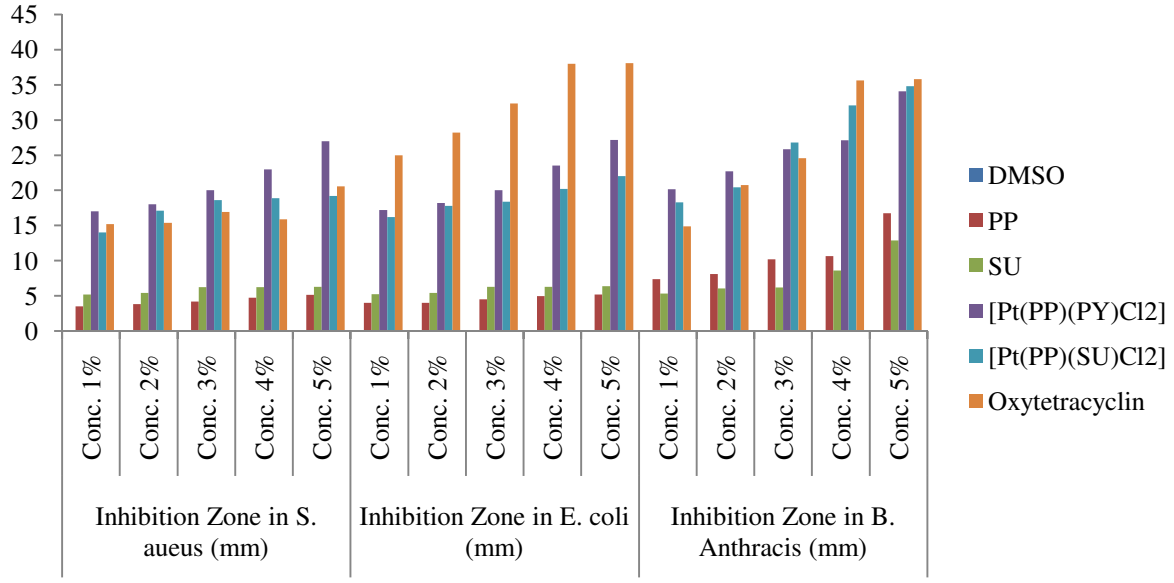


Figure-7: Chart showing zones of inhibition of the samples in some selected bacteria strains.

From Table-7 and Figure-7 above, the solvent (DMSO) showed no zone of inhibition confirming non-involvement of solvent on the activity of metal complexes and ligands. The overall results show that both metal complexes have high inhibition potentials

than the parent ligands against the selected organisms at constant experimental conditions, especially against the gram negative *Bacillus anthracis* [2,4,7,10] and compete well with a known antibiotic, oxytetracyclin. The activities of the metal complexes increased remarkably with increase in concentration. This is additional evidence of good antibacterial performance of the synthesized complexes against the selected bacteria strains.

Conclusion

The complexation between $H_2PtCl_6.6H_2O$ and mixed ligands from pyrimethamine, sulfadoxine and piperaquine has been studied. The synthesized Pt metal complexes have been characterized by solubility test, melting point determination, conductivity, elemental analysis, UV-visible spectrophotometry, FTIR, ^{1}H NMR, ^{13}C NMR, DEPT-135 and XRD spectroscopy. FTIR spectral data showed that all the ligands behaved as bidendate ligands while electronic spectral and magnetic studies suggested octahedral geometry around metal ion. The NMR and XRD results provided supporting evidences of coordination and the nature of the crystals formed. The screening data of antibacterial studies revealed that the metal complexes exhibited enhanced activities than the free ligands indicating that they are more efficient antibacterial agents. The synthesised metal complexes were equally shown to have encouraging antioxidant activity. This study may lead to discovery of new chemotherapeutic antioxidants/antibacterial agents that are metal based.

Acknowledgement

Appreciation to Cape Pennisula University of Technology, South Africa, The Concord School, Ibadan, Nigeria, Kwara State University, Malete, Nigeria, Stellenbosch University, South Africa, iThemba Scientific Lab, South Africa for providing workspaces and analysis.

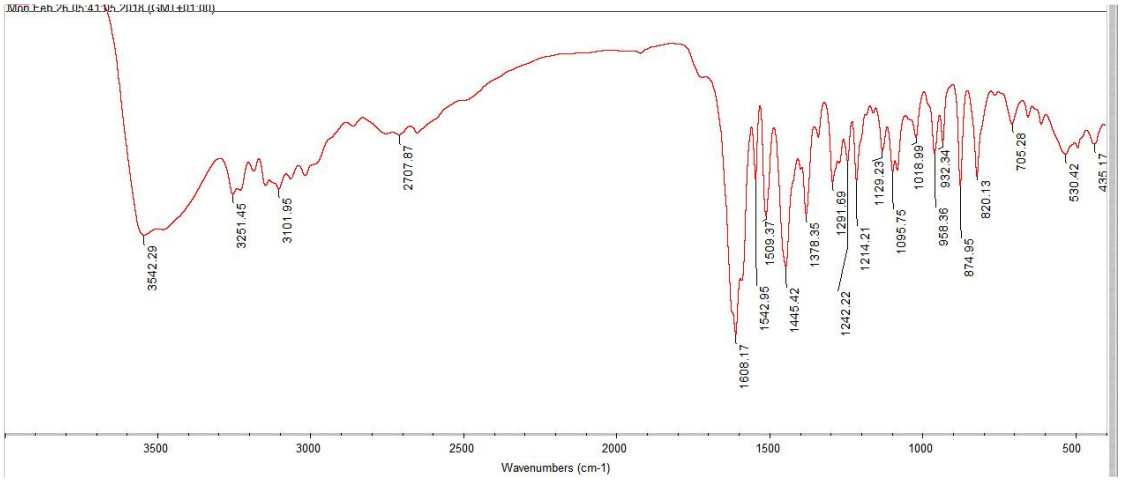


Figure-1: FTIR spectrum of $[Pt(PP)(PY)Cl_2]$

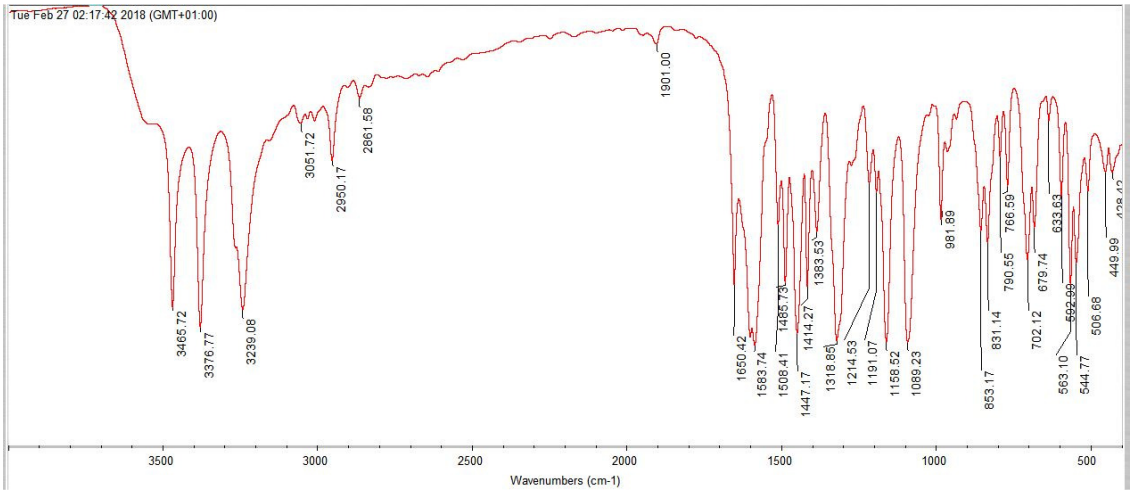


Figure-2: FTIR spectrum of $[Pt(PP)(SU)Cl_2]$

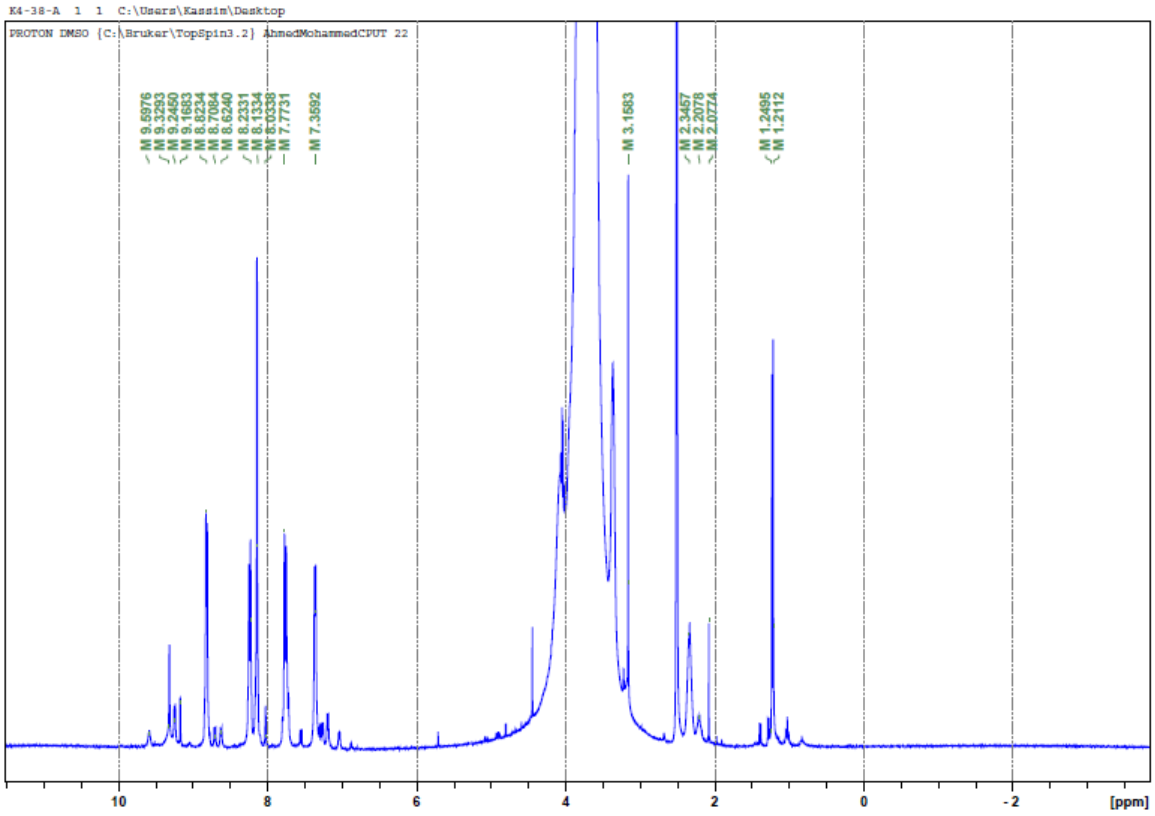


Figure-3: ^{1}HNMR spectrum of [Pt(PP)(PY)Cl_2].

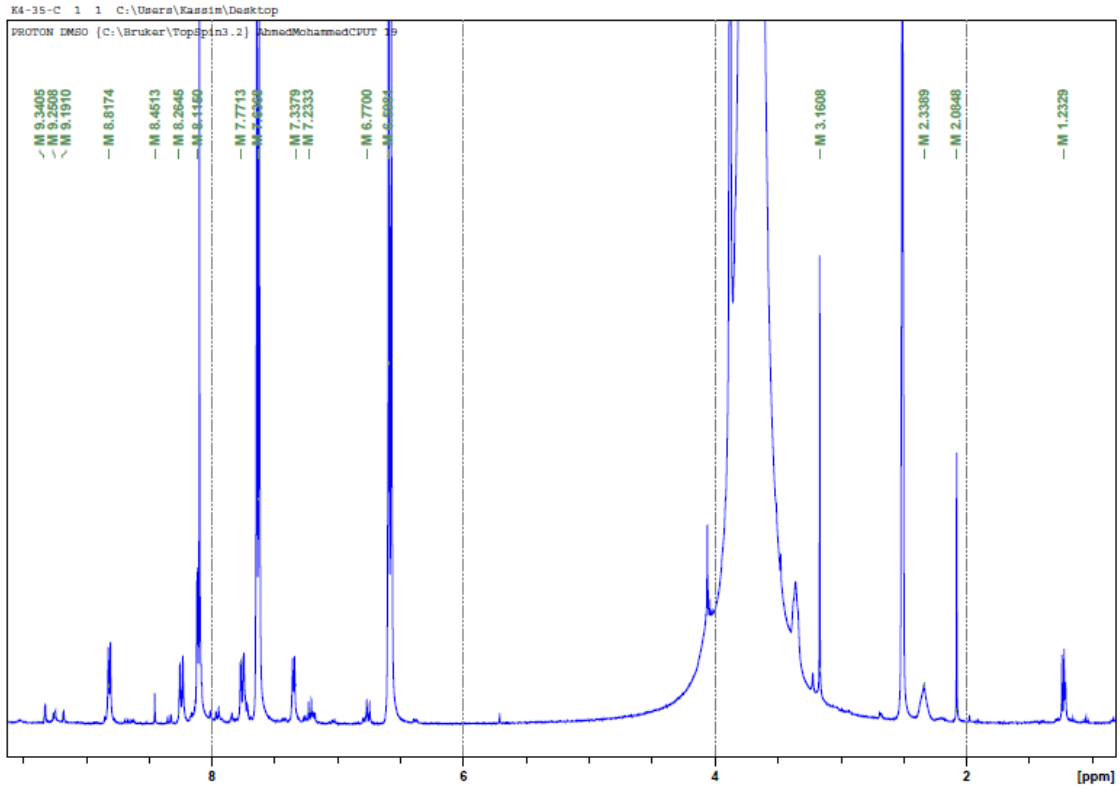


Figure-4: ^{1}HNMR spectrum of [Pt(PP)(SU)Cl_2].

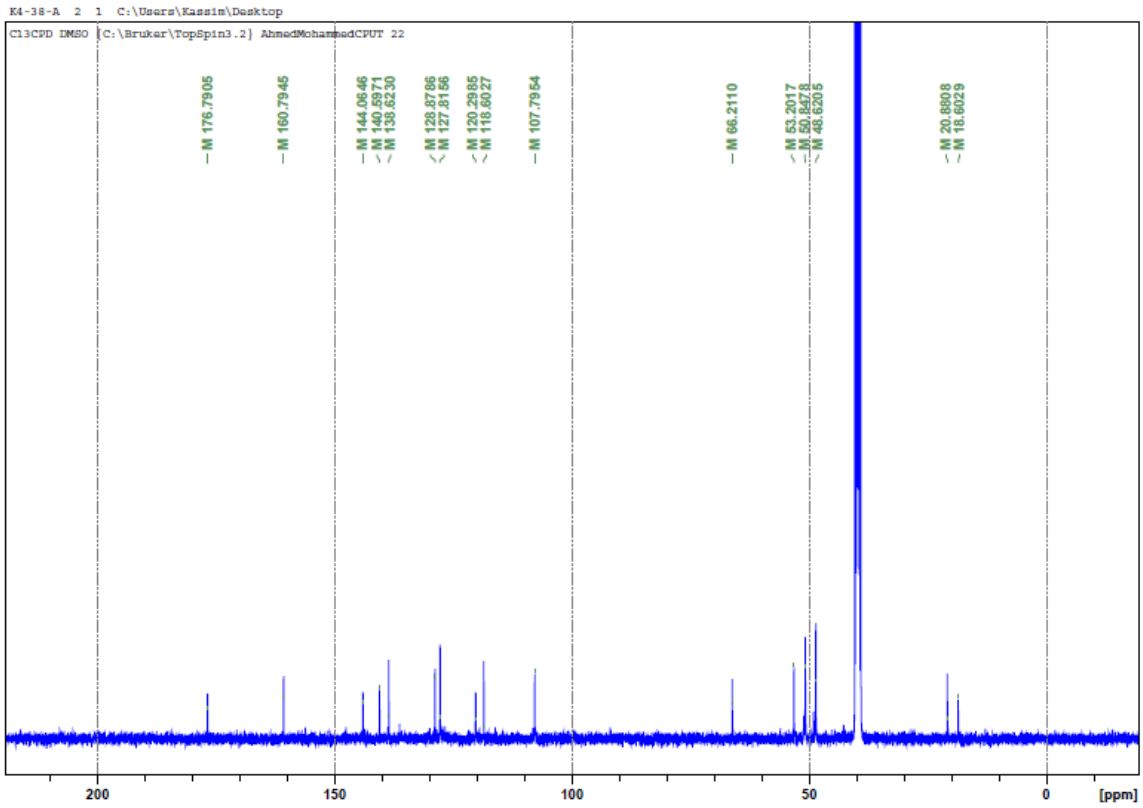


Figure-5: ^{13}C NMR of $[Pt(PP)(PY)Cl_2]$.

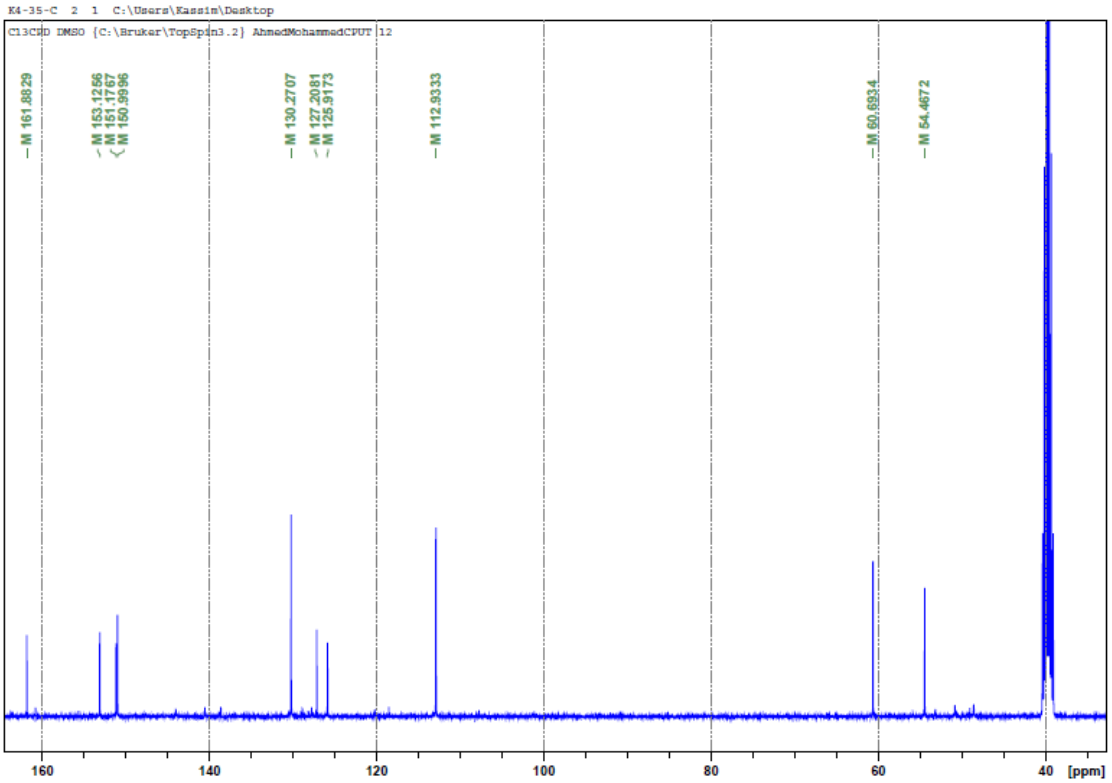


Figure-6: ^{13}C NMR of $[Pt(PP)(SU)Cl_2]$.

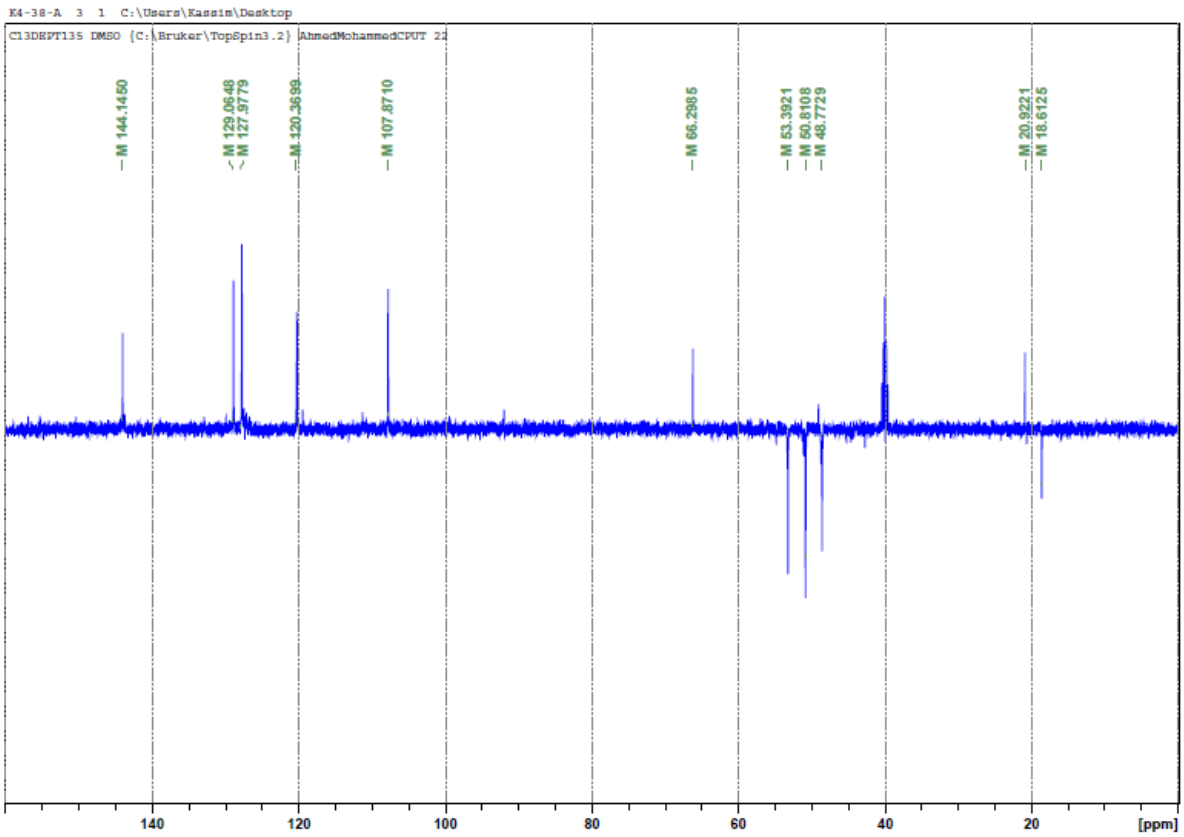


Figure-7: DEPT-135 of [Pt(PP)(PY)Cl_2].

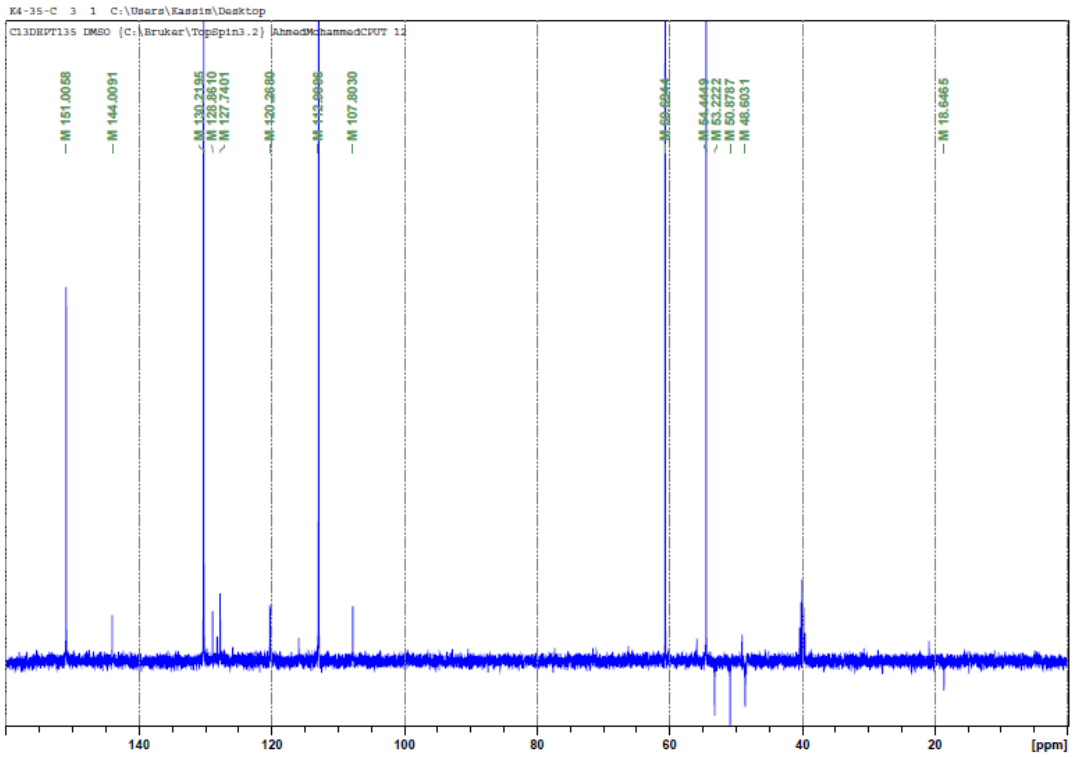


Figure-8: DEPT-135 of [Pt(PP)(SU)Cl_2].

Table-8: Elemental Analysis.

ICP-MS Laboratory CAF Central Analytical Facilities STELLENBOSCH UNIVERSITY Agilent Technologies Authorized Partner Laboratory

	Name	*Weight (mg)*	N [%]	C [%]	H [%]	S [%]
QC value	Cert Ref Std sulfamethazine		20,13	51,78	5,07	11,52
	QC Analysed	4.611	19.82	50.94	4.947	11.483
	%Recovery calculated		*#VALUE!*	*#VALUE!*	*#VALUE!*	*#VALUE!*
	Umar_ A(PP-Pt-SU)	4.6160	8.69	30.54	4.35	1.99
	Umar_ C (PP-Pt-PY)	5.5320	9.30	30.36	4.26	0.00
	Umar_ P	2.2600	0.14	11.43	0.94	0.86
	Umar_ Q (Co-NaD-Pip)	4.1200	9.48	45.21	6.35	0.00
	Umar_ W	6.6780	0.18	25.50	4.36	6.12
	Umar_ X (Cu-NaD-Pip)	3.6200	6.80	45.21	6.35	0.00

References

1. Joel T. (2007). Piperaquine: Bioanalysis, Drug Metabolism and Pharmacokinetics. *Elsevier Ltd, American Society for Pharmacology and Experimental Therapeutics (ASPET), and American Society for Microbiology*, 1, 1-71. ISBN: 978-91-628-7233-5
2. Ayipo Y.O., Obaleye J.A. and Badeggi U.M. (2017). Novel metal complexes of mixed piperaquine-acetylsalicylic acid; synthesis, characterization and anti microbial activities. *J.Turkishchemical society,* 4(1), 313-326. http://dx.doi.org/10.18596/jotcsa.287331
3. Pubchem Open Chemistry Data base (2018). Piperaquine, Sulfadoxine, Pyrimethamine. https://pubchem.ncbi.nlm.nih.gov/compound/
4. Shruti S.S., Jadhav W.N., Khade B.C. and Arbad B.R. (2014). Synthesis, Characterization and Antimicrobial Study of Some 3d Metal Complexes of Sulfadoxine. *International Journal of ChemTech Research,* 6(4), 2291-2294. http://www.sphinxsai.com/framesphinxsaichemtech.htm
5. Thaitong S. (1983). Clones of different sensitivities in drug resistant isolates of plasmodium Falciparum. *J. Bull W.H.O*, 61(4), 709-712. www.malariaresearch.eu
6. Rafique S., Idrees M., Nasim A., Akbar H. and Athar A. (2010). Transition metal complexes as potential therapeutic agents. *J. Biotechnol. Mol. Biol. Rev*., 5(2), 38-45. http://www.academicjournals.org/BMBR
7. Adedeji J.F., Olayinka E.T., Adebayo M.A. and Babatunde O. (2009). Antimalarial mixed ligand metal complexes: synthesis, physicochemical and biological and biological activities. *J.phys.sci*., 4(9), 529-534. http://www.academicjournals.org/ijps
8. Peter A. A. and Gabriel K. (2008). Synthesis, characterization, antiplasmodial and antitrypanosomal activity of some metal(III) complexes of sulfadiazine. *Bulletin of the Chemical Society of Ethiopia,* 22(2), 261-268. DOI: 10.4314/bcse.v22i2.61295
9. Varbanov H., Valiahdi S.M., Legin A.A., Jakupec M.A., Roller A., Galanski M. and Keppler B.K. (2011). Synthesis and characterization of novel bis (carboxylato) dichloridobis (ethylamine) platinum (IV) complexes with higher cytotoxicity than cisplatin. *European journal of medicinal chemistry*, 46(11), 5456-5464. 10.1016/j.ejmech.2011.09.006
10. Osunniran W.A., Obaleye J.A., Ayipo Y.O., Rajee A.O. and Enemose E.A. (2018). Six Coordinate Transition Metal (II) Complexes of Mixed Ligands of Eflornithine Hydrochloride Hydrate and 2, 2-Bipyridine: Synthesis, Characterization and Antibacterial Study. *Jordan Journal of Chemistry*, 13(3), 149-157.
11. Egan T.J., Koch K.R., Swan P.L., Clarkson C., Van Schalkwyk D.A. and Smith P.J. (2004). In vitro antimalarial activity of a series of cationic 2, 2 '-bipyridyl-and 1, 10-phenanthrolineplatinum (II) benzoylthiourea complexes. *Journal of medicinal chemistry*, 47(11), 2926-2934. https://pubs.acs.org/doi/abs/10.1021/jm031132g
12. Kasˇparkova J., Novakova O., Vrána O., Intini F., Natile G. and Brabec V. (2006). Molecular aspects of antitumor effects of a new platinum (IV) drug. *Molecular pharmacology*, 70(5), 1708-1719. 10.1124/mol.106.027730

13. Jeffery G.H., Bassett J., Mendham J. and Denney R.C. (1989). Quantitative Chemical Analysis. 5th Ed., *John Wiley & Sons Inc., New York*, 339, 480-485.

14. Cervato G., Carabelli M., Gervasio S., Cittera A., Cazzola R. and Cestaro B. (2000). Antioxbdant properties of oregano (Origanum vulgare) leaf extracts. *Journal of Food Biochemistry*, 24(6), 453-465. https://onlinelibrary.wiley.com/doi/abs/ 10.1111/j.1745-4514.2000.tb00715.x

15. Obaleye J.A., Amolegbe S.A. and Gbotoso G.O. (2006). Synthesis and characterization of some metal complexes against malaria parasite. *J.Sci & National Development.,* 114-119.

16. Majthoub A., Elsewedy E.M., El-Sayed M.Y., Adam A.M. A. and Refat M.S. (2017). Synthesis of New Cadmium (II) Antipyretic Drug. *research journal of pharmaceutical biological and chemical sciences*, 8(1), 639-645. ISSN: 0975-8585.

17. Gupta H.K. and Dikshit S.K. (1985). Palladium (II), platinum (II) and platinum (IV) complexes of 2-mercapto-3-phenyl-4-quinazolinone: Reactions of palladium (II) chloride and platinum (IV) chloride with 2-mercapto-3-phenyl-4-quinazolinone in the presence and absence of variousN-heterocyclic bases. *Transition Metal Chemistry*, 10(12), 469-472.

18. Miessler G.L., Fischer P.J. and Tarr D.A. (2014). Inorganic Chemistry 5th Edition. *Pearson Educ. Inc., USA*, 314-320. ISBN-13: 978-0-321-81105-4

19. Pavia D.L., Lampman G.M. and Kriz G.S. (2001). Introduction to Spectroscopy 3rd Edition. *Thomson Learning Inc., USA*, Page 29, 109-152, 167-189, 357. ISBN: 0-03-031961-7

20. Swihart D.L. and Mason W.R. (1970). Electronic Spectra of Octahedral Platinum (IV) Complexes. *Inorg. Che.,* 9 (7), 1749-1757. DOI: https://doi.org/10.1021/ic50089a029

21. Kunkely H. and Vogler A. (1991). Transition Metal and Rare Earth Compounds. *Inorg. Chim Acta,* 186, 155, 90. DOI: 10.1007/3-540-44447-5

22. Al-Adilee K. and Dakheel K. (2018). Synthesis, Spectral and Biological Studies of Ni(II), Pd(II) and Pt(IV) Complexes with New Heterocyclic ligand Derived from Azo-Schiff Bases Dyes. *Eurasian J. Anal Chem,* 13(5), em64. https://doi.org/10.29333/ejac/97267

23. Al-Hazmi A., Warren J., Amartey S.S. and Qin W. (2014). Discovery, Modification and Production of L4 Lysozyme for Industrial and Medical Uses. *International Journal of Biology*, 6(4), 9. https://doi.org/10.5539/ ijb.v6n4p45

24. Jain P.K., Ghosh D., Baer R., Rabani E. and Alivisatos A. P. (2012). Near-field Manipulation of Spectroscopic Selection Rules on Nanoscale. *PNAS*, 109(21), 8016- 8019. https://doi.org/10.1073/ pnas.1121319109

25. UCI. (2018). Crystal Structure Analysis: X-ray diffraction, Electron diffraction, Neutron diffraction, Essence of diffraction: Bragg's diffraction, Reading. *West 5, A/M 5-6, G/S 3*. https://www.chem.uci.edu/~lawm/263%204.pdf

26. Speakman S.A. (2018). Estimating crystallite size using XRD. *MIT Centre for materials science and engineering,* 3-8. http://prism.mit.edu/xray

27. Falak S. (2010). Crystal Structure Determination I, Pakistan Institute of Engineering and Applied Science. *Khwarzimi Science Society.* www.khwarzimic.org

28. Bragg's Law (2018). Braggs. xlsx. www.ccp14.ac.uk/ ccp/bca-spreadsheets

29. Gavhane V.S., Rajbhoj A.S. and Gaikwad S.T. (2015). X-ray Diffraction Study and Biological Analysis of Transition Metal Complexes of N-4-Disubstituted Thiosemicrbazone. *Research Journal of Chemical Sciences*, 5(12), 33-37. www.isca.in

30. Rigaku (2018). Integrated X-ray powder diffraction software for more advanced analysis. *Rigaku PDXL XRD analysis software.pdf.* www.rigaku.com/service/pdxl

31. Touchstone (2018). X-ray Diffraction (XRD) Analysis. *INOVATIA.* https://thegoodinside.com/wp-content/uploads/ X-ray_Diffraction_Analysis.pdf

32. Hussain R. and Juneja H.D. (2009). X-Ray Diffraction Studies of Some Chelate Polymers of Adipic Acid. *Int. J. Chem. Sci.,* 7(2), 632-638. https://www.tsijournals.com/ artiles

33. Ukey V.V., Rewatkar K.G., Borkar S.D., Bonde A.D., Naz S. and Juneja H.D. (2005). X-Ray Diffraction Studies of Some Chelate Polymers of Hydroxamic Acid. *Int. J. Chem. Sci.,* 5(2), 229-236. https://www.tsijournals.com/ artiles

34. Garg A. and Gurao N. (2018). X-ray Diffraction: Principles and Practice. *Department of Materials Science and Engineering, Indian Institute of Technology, Kanpur.* https://www.iitk.ac.in/XRD_AGNPG

35. Qing W., Yan M., Xin L., Shan L. and Hu L. (2015). X-ray powder diffraction data of piperaquine. *Camb. Core J. Powder Diffraction,* 30(3), 289-292. https://doi.org/10.1017/S0885715615000524

36. Hyde T. (2008). Crystallite Size Analysis of Supported Platinum Catalyst by XRD. *Platinum Metals Rev.,* 52(2), 129-130. DOI: https://doi.org/10.1595/ 147106708X299547

37. Badakhshan M.P., Subramanion L.J., Lachimanan Y.L., Yeng C. and Sreenivasan S. (2012). Antioxidant Activity of Methanol Extracts of Different Pats of *Lantana camara. Asian Pac J Trop Biomed,* 2(12), 960-965. https://dx.doi.org/10.1016%2FS2221-1691(13)60007-6

38. Naima S., Muhammad R.K. and Maria S. (2012). Antioxidant activity, total phenolic and total flavonoid contents of whole plant extract *Torilis leptophylla L. BMC*

Complement Altern Med., 12, 221. https://doi.org/10.1186/ 1472-6882-12-221